Design, Simulation, and Testing of an S-Band Coaxial Multipactor Test-Cell

Stephen V. Langellotti, Nicholas M. Jordan, Y. Y. Lau, and Ronald M. Gilgenbach
Plasma, Pulsed Power, and Microwave Laboratory
Department of Nuclear Engineering and Radiological Sciences
University of Michigan
Ann Arbor, MI, USA

Abstract: *In satellite communication systems, multipactor discharges have the potential to disrupt signal transmission and damage hardware. This paper discusses the design, simulation, and testing of a coaxial multipactor test-cell that will be operated at GHz frequencies. The experiment's design has been guided by CST Particle Studio PIC simulations to predict multipactor breakdown. A number of diagnostic instruments will be used to detect and characterize the discharge. This experiment will ultimately be used to study the multipactor phenomenon and explore mitigation strategies.*

Keywords: multipactor; coaxial; satellite

Introduction

Multipactor is a discharge phenomenon that can result in disruption in microwave transmission [1, 2], degradation of signal quality [3], and even catastrophic damage to the device [2, 4]. In the coaxial geometry, multipactor is very difficult to study analytically [3] and there is limited experimental data in the public domain [5, 6]. Because of this, it is challenging to predict multipactor onset. Multipactor is of particular concern in satellite communications because it is impossible to repair or replace damaged components. As a result, it is necessary to build devices with large safety margins, leading to increased costs and reduced performance.

This paper presents the design of a test-cell for studying multipactor in a coaxial geometry. The test-cell will be used to measure the multipactor breakdown threshold and test various surface treatments and other mitigation strategies.

Multipactor Simulations

The coaxial test-cell was designed based on PIC code simulations in CST Particle Studio [7]. A cross-sectionional representation of the simulation geometry is shown in Fig. 1. At the center of the test-cell is the multipacting region. The outer conductor has a diameter of 19.1 mm. The gap between the inner and outer conductors in the multipacting region is $d = 1.59$ mm. The simulation volume is bounded by two 50 Ω wave ports. Quarter-wave transformers on either side of the multipacting region ensure an impedance match between the wave ports and the multipacting region. The stepped impedance transformers also provide isolation of the multipacting region from the rest of the transmission line. Since the gap spacing is much larger in the 50 Ω coaxial segments, the multipactor threshold voltage is much higher. Thus, multipactor should only occur in the central, multipacting region.

Work supported by AFOSR MURI Grant No. FA9550-18-1-0062 through Michigan State University and by L3Harris Electron Devices Division.

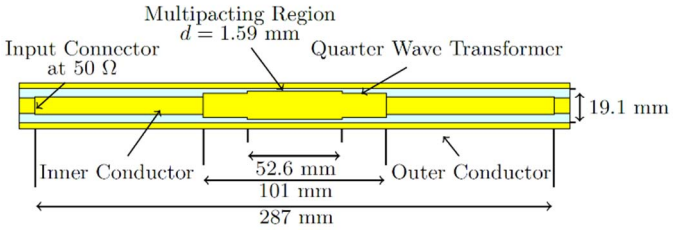

Fig. 1: Cross-section of the coaxial test-cell simulation geometry.

The multipactor threshold was determined by seeding the multipacting region with 10^4 electrons. These seed electrons have random position, direction, and energy. A 3.05 GHz TEM wave is supplied from one of the wave ports with a voltage, V_{rf}. The multipactor threshold is determined by sweeping the applied RF voltage and measuring the growth of the electron population as a function of time. The minimum threshold for multipactor occurs when the electron population is neither increasing nor decreasing. When this procedure is applied to our simulation geometry, we obtain the susceptibility diagram shown in Fig. 2. For the designed gap spacing, (1.59 mm, $f \times d = 4.84$ GHz mm), breakdown is predicted to occur at 298 V and 4.1 kW. The secondary emission yield was modeled using data for chemically cleaned copper [8].

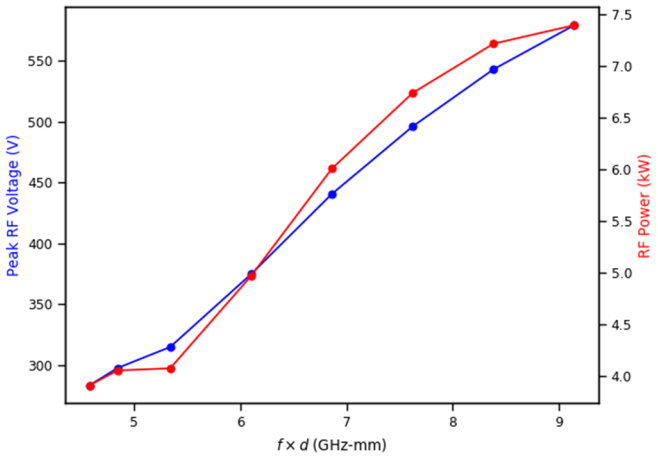

Fig. 2: Simulated susceptibility diagram for the experimental geometry.

Experimental Configuration

The test-cell consists of a coaxial transmission line suspended in a vacuum chamber, as shown in Fig. 3. The basic dimensions of this transmission line are the same as in the schematic in Fig. 1. The inner and outer conductor are both constructed from oxygen-free high-purity copper. A number of

small, 1 mm diameter, holes in the outer conductor surround the multipacting region and provide for the placement of optical fibers and diagnostics. Additional 3 mm holes are placed over the 50 Ω segments to improve vacuum conductance. A MIGHTEX fiber-coupled LED source provides 265 nm ultraviolet light for electron seeding. Additional optical fibers are coupled to an external photomultiplier tube for detection of light emissions. An electron multiplier tube placed outside the transmission line provides direct detection of the multipactor electrons.

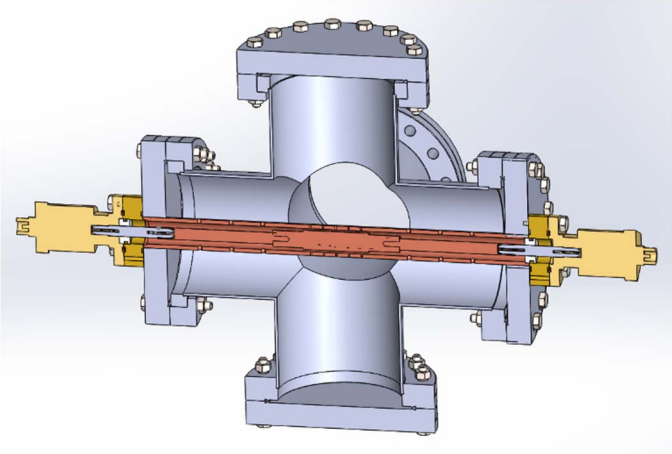

Fig. 3: CAD rendering of the experimental transmission line with gas barrier and N-type connectors.

Microwave power is supplied from an external 30 kW magnetron at 3.05 GHz. Directional couplers provide power measurements at the input and output of the chamber. MYAT gas barrier flanges act as RF windows to couple power into the chamber. Rigid coax feedthrough couplers adapt the test-cell transmission line to external N-type connections.

The test-cell is currently undergoing testing of its multipactor generation capabilities. The diagnostics are being refined and tested to ensure accurate measurement of the multipactor discharges. Future work includes testing various mitigation strategies and characterizing the multipactor discharge.

We also plan to test the CST code against the Ramo-Shockley Theorem [9, 10] which has been extensively used to account for the induced current by the motion of a multipactoring electron, particularly when the electron is about to hit a surface.

References

[1] R. A. Kishek, Y. Y. Lau, L. K. Ang, A. Vafells, and R. M. Gilgenbach, "Multipactor Discharge on Metals and Dielectrics: Historical Review and Recent Theories," *Phys Plasmas*, vol. 5, no. 5, pp. 2120–2126, Jan. 1998.

[2] J. R. M. Vaughan, "Multipactor," *IEEE T Electron Dev*, vol. 35, no. 7, pp. 1172–1180, Jul. 1988.

[3] P. Y. Wong, Y. Y. Lau, P. Zhang, N. Jordan, R. M. Gilgenbach, and J. Verboncoeur, "The Effects of Multipactor on the Quality of a Complex Signal Propagating in a Transmission Line," *Phys Plasmas*, vol. 26, no. 11, Nov. 2019, Art. no. 112114.

[4] J. R. M. Vaughan, "Some high-power window failures," *IRE T Electron Dev*, vol. 8, pp. 302–308, Jul. 1961.

[5] R. Woo, "Multipacting Discharges between Coaxial Electrodes," *J Appl Phys*, vol. 39, no. 3, pp. 1528–1533, Sep. 1968.

[6] T. P. Graves, "Experimental Investigation of Electron Multipactor Discharges at Very High Frequencies," PhD Thesis, Massachusetts Institute of Technology, 2006.

[7] *CST Studio Suite*. (2019), Dassault Systems.

[8] I. Bojko, N. Hilleret, and C. Scheuerlein, "Influence of Air Exposures and Thermal Treatments on the Secondary Electron Yield of Copper," *J Vac Sci Tech A*, vol. 18, no. 3, pp. 972–979, Mar. 2000.

[9] S. Ramo, "Currents Induced by Electron Motion," *Proc. I.R.E.*, vol. 27, pp. 584–585, Sep. 1939.

[10] W. Shockley, "Currents to Conductors Induced by a Moving Point Charge," *J. Appl. Phys.*, vol. 9, pp. 635–636, May 1938.